Analytic vortices and magnetic resonances in rotating superfluid ^{3}He-A. III

Xenophon Zotos and Kazumi Maki
Department of Physics, University of Southern California, Los Angeles, California 90089-0484
(Received 1 November 1983)

We study variationally the circular-hyperbolic vortex-pair free energy. This bound pair yields a free energy much lower than that from a pair of isolated analytic vortices. The satellite resonance frequency of the pure $\hat{l}$ vortex pair and that of the vortex pair with nonuniform $\hat{d}$ are analyzed. We find that the pure $\hat{l}$ vortex pair gives the observed transverse satellite frequency as well as the observed intensity of the satellite, while the vortex pair with nonuniform $\hat{d}$ gives a satellite frequency that is somewhat lower than observed experimentally. It is puzzling why the pure $\hat{l}$ vortex with higher free energy than that from the vortex with nonuniform $\hat{d}$ is more consistent with experiment.

I. INTRODUCTION

In a series of papers[1,2] (which will be referred as I and II, respectively) we have studied the spatial conformation of three types of analytic vortices and associated satellite frequencies in rotating superfluid ^{3}He-A, which can in principle be compared with the experimental data by Hakonen *et al.*[3,4] We found that the vortex lattice formed by the circular and the hyperbolic vortices is most stable, which is the generalization of the result obtained by Fujita *et al.*[5] However, such a vortex lattice has two separate satellite resonances, in contradiction to the experimental observation[3,4] in rotating ^{3}He-A. Furthermore, the apparent agreement between the average satellite resonance frequency and the observation[2] is fortuitous. Better variational solutions for the analytic vortices give the satellite frequencies much closer to the bulk resonance frequency. The details of this analysis will be summarized in Appendix A.

More recently the NMR experiment is performed in a tilted magnetic field from the rotation axis. No apparent change in the satellite frequency has been observed.[6] This experimental result eliminates the type of analytic vortices studied in I and II as possibilities in the observations of the rotating ^{3}He-A experiment.

The only texture which is insensitive to the orientation of the static magnetic field is mostly made of the $\hat{l}$ texture. A model which fulfills this constraint has been already proposed by Seppälä and Volovik[7] (SV). They described this vortex as a variant of a 4π analytic vortex[8] of pure $\hat{l}$ texture. A more precise description of this texture, however, is the bound pair of two 2π analytic vortices. The type of vortex studied by SV is the bound state of a radial and hyperbolic vortex, while we shall show that the bound state of the circular and hyperbolic vortex gives a lower vortex free energy.

The spatial conformations of the $\hat{l}$ vector projected on the x-y plane for these two types of vortices are sketched in Figs. 1(a) and 1(b), respectively. Since the circular-hyperbolic variety of the SV vortex has the lower energy, we shall limit ourselves to this texture. In Sec. II we analyze a pure $\hat{l}$ texture of the circular-hyperbolic SV vortex. We find that the spatial conformation of the analytic vortex depends weakly on r_0, the cutoff distance. Then, limiting ourselves to the parallel geometry where $\vec{H}||\vec{\Omega}$ ($\vec{H}$ is the static magnetic field and $\vec{\Omega}$ is the rotation vector of the cylinder containing superfluid ^{3}He-A), we analyze in Sec. III the effect of nonuniform $\hat{d}$. We find that introduction of nonuniform $\hat{d}$ produces a somewhat extended texture with lower free energy than the pure $\hat{l}$

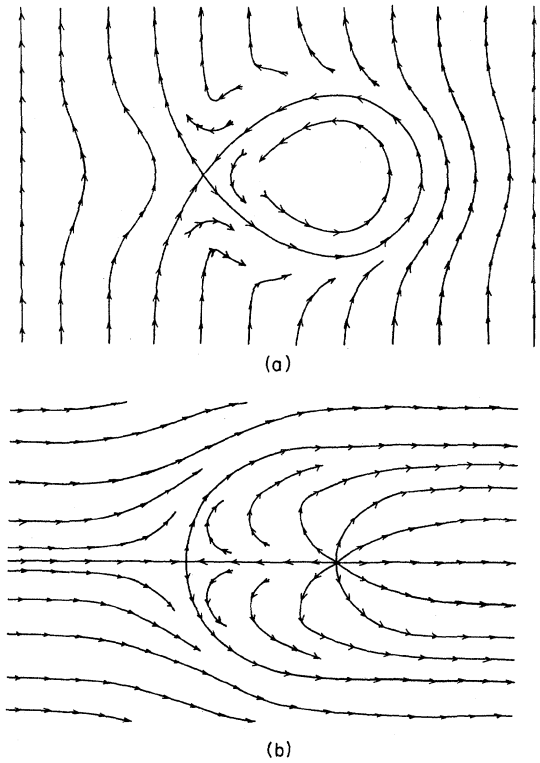

FIG. 1. $\hat{l}$ textures associated with 2π vortex-pair configurations projected in the $\hat{x}$-$\hat{y}$ plane are sketched. The arrows indicate the $\hat{l}$ direction: (a) the circular-hyperbolic pair and (b) the radial-hyperbolic pair.

vortex. Now the spatial conformations of $\hat{l}$ and $\hat{d}$ are independent of r_0 as long as $r_0 > 5\xi_\perp$, where $\xi_\perp$ ($\simeq 10\ \mu$m) is the dipole coherence length. We analyze the associated satellite resonance frequencies in Sec. IV. The transverse satellite frequency of the pure $\hat{l}$ texture agrees quite well with the observed satellite frequency in the rotating ^{3}He-A extrapolated to $T=T_c$, although the observed satellite frequency does not exhibit any appreciable r_0 dependence (i.e., Ω dependence) contrary to this model. On the other hand, the texture with nonuniform $\hat{d}$ vector gives the transverse satellite frequency somewhat below the one observed experimentally. At present it seems that the pure $\hat{l}$ vortex is more consistent with the experimental results, although it has a higher free energy than the nonuniform $\hat{d}$ vortex, and further work is necessary to clarify this discrepancy. By a similar analysis for the radial-hyperbolic SV vortex in Appendix B, we find that the corresponding transverse resonance frequency is much lower than that of the circular-hyperbolic SV vortex.

II. PURE $\hat{l}$ VORTEX

The observed insensitivity of the satellite resonance frequency to the magnetic field orientations suggests strongly that the texture involved is the pure $\hat{l}$ texture. We shall study in this section the pure $\hat{l}$ texture corresponding to the circular-hyperbolic SV vortex within the Ginzburg-Landau approximation. As in I we shall start with the vortex free energy per unit length:

$$
\begin{aligned}
f=\frac{A}{2}\int d^2r\,[&4[\vec{\nabla}\alpha+\cos\beta(\vec{\nabla}\gamma)]^2+3\sin^2\beta(\vec{\nabla}\gamma)^2\\
&-2\sin^2\beta\{[(\cos\gamma)\alpha_n-(\sin\gamma)\alpha_y]^2+[(\sin\gamma)\gamma_x+(\cos\gamma)\gamma_y]^2\}+(\vec{\nabla}\beta)^2+2\sin^2\beta[(\cos\gamma)\beta_x-(\sin\gamma)\beta_y]^2\\
&+4\sin\beta[(\cos\gamma)\beta_x-(\sin\gamma)\beta_y]\{\sin\gamma[\alpha_x+(\cos\beta)\gamma_x]+\cos\gamma[\alpha_y+(\cos\beta)\gamma_y]\}\\
&+2((1+\cos^2\beta)\,|\,\vec{\nabla}\chi\,|^2+\sin^2\beta[(\sin\gamma)\chi_x+(\cos\gamma)\chi_y]^2\\
&\quad+\sin^2\chi[(1+\cos^2\beta)\,|\,\vec{\nabla}\psi\,|^2+\sin^2\beta[(\sin\gamma)\psi_x+(\cos\gamma)\psi_y]^2])\\
&+4\xi_\perp^{-2}\{1-[\cos\chi\cos\beta+\sin\chi\sin\beta\cos(\gamma-\psi)]^2\}]\ ,
\end{aligned}
\tag{1}
$$

where α, β, and γ are the Euler angles describing the orientation of $\hat{l}$ and $\hat{\Delta}$ as

$$
\begin{aligned}
\hat{l}&=\sin\beta[-(\cos\gamma)\hat{x}+(\sin\gamma)\hat{y}]+(\cos\beta)\hat{z}\ ,\\
\hat{\Delta}&=e^{i\alpha}\{\cos\beta[(\cos\gamma)\hat{x}-(\sin\gamma)\hat{y}]+(\sin\beta)\hat{z}\\
&\quad+i[(\sin\gamma)\hat{x}+(\cos\gamma)\hat{y}]\}\ ,
\end{aligned}
\tag{2}
$$

while χ and ψ describe the orientation of $\hat{d}$,

$$
\hat{d}=\sin\chi[-(\cos\psi)\hat{x}+(\sin\psi)\hat{y}]+(\cos\chi)\hat{z}\ , \tag{3}
$$

and $\xi_\perp$ is the dipole coherence length. We shall consider a pure $\hat{l}$ texture with a uniform $\hat{d}$ vector. We shall take the direction of $\hat{d}$ in the $\hat{y}$ direction, which gives

$$
\chi=\psi=\frac{\pi}{2}\ . \tag{4}
$$

More generally when the static field $\vec{H}$ and the rotation vector $\vec{\Omega}$ are not parallel to each other, the uniform $\hat{d}$ direction can be taken to be parallel to $\vec{\Omega}\times\vec{H}$. Since we are interested in the circular and hyperbolic vortex pair, α and β are given by

$$
\alpha=\phi_1+\phi_2,\quad \gamma=-\phi_1+\phi_2+\frac{\pi}{2}\ , \tag{5}
$$

with

$$
\phi_1=\tan^{-1}\left[\frac{y}{x-c}\right],\quad \phi_2=\tan^{-1}\left[\frac{y}{x+c}\right] \tag{6}
$$

corresponding to the circular vortex at $(c,0)$ and the hyperbolic vortex at $(-c,0)$. On the other hand we determine β variationally, choosing

$$
\cos\beta==(\cos v)f(u)\ , \tag{7}
$$

where we have introduced hyperbolic coordinates by

$$
\begin{aligned}
x&=C\cosh u\cos v\ ,\\
y&=C\sinh u\sin v\ .
\end{aligned}
\tag{8}
$$

Substituting Eqs. (4), (5),and (7) into Eq. (1), we can recast Eq. (1) as

$$
f_v=\pi A[I_1(f)+I_2(f)+4\xi_\perp^{-2}I_4(f)]\ , \tag{9}
$$

where

$$
\begin{aligned}
I_1(f)=12u_0-24\ln 2-2+32\int_0^\infty du\,\Bigg[&\frac{1-e^{-u}\cosh^2 uf}{\sinh u\cosh u}-12\int_0^\infty du\left[\frac{1-\cosh^2 uf^2}{\sinh u\cosh u}+f^2\right]\\
&-\int_0^\infty du(5-10e^{-2u}+9e^{-4u}-8\tanh u)f^2\Bigg]\ ,
\end{aligned}
\tag{10}
$$

$$I_2(f)=\int_0^\infty du\{[(1-f^2)^{-1/2}-1]f_u^2f^{-2}+1-(1-f^2)^{1/2}\}$$
$$+\frac{1}{\pi}\int\int du\,dv\sin^2v(\cosh u-\cos v)^2X^{-3}\{[(\cosh u-\cos v)\cosh u-2]\cos v f_u$$
$$+[(\cosh u-\cos v)\cos v+2]\sinh u f\}^2\,, \tag{11}$$

$$I_4(f)=\tfrac{1}{2}C^2\left[\int_0^\infty du(\sinh^2u+\tfrac{1}{4})f^2+4(u_0-2\ln 2+\tfrac{1}{2})-\int_0^\infty du\,e^{-2u}f^2\right], \tag{12}$$

and

$$u_0=\ln(2r_0/C)\,,$$
$$X=\sinh^2u+\sin^2v\,. \tag{13}$$

The details of derivation are given in Appendix C.

Here we cut off the integral at a circle of radius r_0, where r_0 is the average intervortex distance defined by

$$r_0=(\pi n_v)^{-1/2}=(h/2\pi m\Omega)^{1/2}\,. \tag{14}$$

n_v is the vortex density, m is the mass of ^{3}He atom, and Ω is the rotation speed. The $\ln r_0$ divergence of $I_1(f)$ is due to the circulation of the 4π vortex. Within the present approximation (i.e., the uniform $\hat{d}$ vector), the dipole energy term $I_4(f)$ diverges also logarithmically with r_0, which leads to the extra logarithmic dependence of the $\hat{l}$ texture. Finally $f(u)$ is determined variationally assuming

$$f(u)=e^{-a(\cosh u-1)}\,. \tag{15}$$

This particular choice is suggested from our analysis of the isolated analytic vortex as described in Appendix A. This form of the variational function gives the best results for the circular vortex. Then the free energy is minimized for the parameters a and C. The best choices for a and C for given r_0 are shown in Table I. From the table we see that a and C as well as free energy depend weakly on r_0. In any case the vortex free energy thus determined is much lower than that for the isolated vortex discussed in I and II, simply because there is no extra logarithmic term arising from the singularity in the $\hat{d}$ texture. Therefore, the present texture is not only consistent with the experiment in a tilted magnetic field, but also the present vortex configuration is much more favored energetically than the type of the vortex lattice considered in I and II.

A similar analysis is carried out for the radial-hyperbolic vortex pair, which has higher energy than that for the circular-hyperbolic vortex pair as expected. This is intuitively plausible since we know that in the case of the isolated vortex the radial vortex has higher energy than the circular vortex.[1,5] The results for the radial-hyperbolic pair are summarized in Appendix B.

III. NONUNIFORM $\hat{d}$ TEXTURE

When $\vec{H}$ and $\vec{\Omega}$ are parallel to each other the $\hat{d}$ vector is free to move around in the x-y plane. Then the $\hat{d}$ vector becomes asymptotically parallel to the $\hat{l}$ vector away from the center of the vortex, which makes the dipolar energy nondivergent. We shall analyze the effect of the nonuniform $\hat{d}$ as follows; we now take $\chi=\pi/2$, but

$$\sin\psi=1-2(\sin^2v)Y^{-1}\,, \tag{16}$$

with

$$Y=\theta^2+\sin^2v\,. \tag{17}$$

The variational function θ has two constraints. First, for large u, θ must approach $\sinh u$, so that $\hat{d}$ becomes parallel to $\hat{l}$ asymptotically. Second, for $u=0$ [i.e., on the straight line connecting $(C,0)$ and $(-C,0)$] $\hat{d}$ is parallel to $\hat{l}$, implying θ diverges as u approaches 0. We shall choose θ as

$$\theta=\sinh u+\frac{(\sinh b)^2}{\sinh u}\,, \tag{18}$$

which satisfies the two constraints listed above. We have also tried somewhat more general variational functions. For example, the second term in Eq. (18) is replaced by $(\sinh b)^{1+p}/(\sinh u)^p$ with p as an additional variational parameter. However, we discovered that by allowing p to be 1.5 we can improve the free energy about a tenth of a percent. Therefore, we do not think this complication is very useful. With this parametrization of $\hat{d}$, we write the vortex free energy as follows:

$$f_v=\pi A[I_1(f)+I_2(f)+I_3(f,b)+4\xi_\perp^{-2}I_4(f,b)]\,, \tag{19}$$

where I_1 and I_2 are the same as given in Eqs. (10) and (11), while I_3 and I_4 are given by

TABLE I. Circular-hyperbolic vortex size parameters a, c, free energy $f=12\ln(r_0/2C)+\Delta f$, satellite resonance frequencies and intensities, for different values of cutoff distance r_0.

r_0	a	$C/\xi_\perp$	Δf	R_t	$(I_t/I_0)/\Omega$	R_l	$(I_l/I_0)/\Omega$
5.0	0.59	0.699	17.615	0.803	0.0387	0.670	0.0357
10.0	0.51	0.542	16.590	0.868	0.0578	0.773	0.0468
20.0	0.47	0.466	16.175	0.898	0.0679	0.822	0.0509
30.0	0.45	0.435	16.011	0.910	0.0698	0.843	0.0509

$$I_3(f,b)=4\int_0^\infty du\left\{\frac{1}{\theta(\theta^2+1)^{1/2}}[\theta_u^2/(1+\theta^2)+1]+2\left[\left[\frac{\theta^2+\frac{1}{2}}{\theta(\theta^2+1)^{1/2}}-1\right]\theta_u^2+\left[\theta^2-\frac{\theta^2+\frac{1}{2}}{\theta}(\theta^2+1)^{1/2}\right]f^2\right]\right\}$$

$$+\frac{4}{\pi}\int\int du\,dv\sin^2v(1-\cos^2v)(\cosh u-\cos v)^2X^{-3}Y^{-2}$$

$$\times\{[(\cosh u-\cos v)\cos v+2]\sinh u\,\theta_u+[(\cosh u-\cos v)\cosh u-2](\cos v)\theta\}^2\,, \tag{20}$$

and

$$I_4(f,b)=\tfrac{1}{2}C^2\left[\int_0^\infty du\,(\sinh^2u+\tfrac{1}{4})f^2+\frac{4}{\pi}\int\int du\,dv\sin^2v[1-(\cos^2v)f^2]X^{-1}Y^{-2}(\theta-\sinh u)^2(\theta\sinh u+\sin^2v)^2\right]. \tag{21}$$

The vortex free energy is now minimized for three parameters a, b, and C. We find that

$$f_v=\pi A[12\ln(r_0/2C)+18.44]\,,$$

with

$$a=0.9,\ b=1.2,\ \text{and}\ C=1.18\xi_\perp\,. \tag{22}$$

The above free energy is substantially lower than the vortex free energy with uniform $\hat{d}$ discussed in Sec. II, since the present C is bigger by a factor of 2 than that of the pure $\hat{l}$ vortex. Furthermore, the second term in Eq. (22) is independent of the cutoff parameter r_0 as long as $r_0\geq 5\xi_\perp$.

Furthermore, the constant C is quite comparable with the recent numerical result by Seppälä[9] on the same texture. On the other hand, his vortex free energy is different from ours, very likely because of the surface integral terms.

The corresponding energy for the radial-hyperbolic vortex pair is given by

$$f_v^{\rm rh}=\pi A[12\ln(r_0/2C)+22.76]\,,$$

with

$$a=0.7,\quad b=1.2,\quad \text{and}\ C=1.11\xi_\perp\,. \tag{23}$$

Therefore, the radial-hyperbolic type definitely has higher energy than that of the circular-hyperbolic vortex.

IV. MAGNETIC RESONANCES

As is the case for the isolated vortex, the present vortex pair allows one spin-wave bound state for each of the transverse and the longitudinal oscillations which couples to the homogeneous magnetic field. There are other modes with the incorrect parity, which do not couple to the magnetic field. The satellite resonance frequencies are determined by the eigenvalues λ_g and λ_f as

$$\omega_t^{\rm sat}=(\omega_0^2+\lambda_g\Omega_A^2)^{1/2}\,,$$
$$\omega_l^{\rm sat}=(\lambda_f)^{1/2}\Omega_A\,, \tag{24}$$

where ω_0 is the Larmor frequency and Ω_A is the Leggett frequency. Here subscripts t and l indicate the transverse and the longitudinal modes. The corresponding eigenvalues are determined from

$$\lambda_g=\int\int dx\,dy(\tfrac{1}{2}\{(1+\cos^2\beta)\,|\,\nabla g\,|^2+\sin^2\beta[(\sin\gamma)g_x+(\cos\gamma)g_y]^2\}$$
$$-g^2\{(1+\cos^2\beta)\,|\,\nabla\psi\,|^2+\sin^2\beta[(\sin\gamma)\psi_x+(\cos\gamma)\psi_y]^2\}+(\sin^2\beta\sin^2\gamma-\cos^2\beta)g^2)\Big/\int dx\,dy\,|\,g\,|^2\,, \tag{25}$$

and

$$\lambda_f=\int dx\,dy(\tfrac{1}{2}\{(1+\cos^2\beta)\,|\,\nabla f\,|^2+\sin^2\beta[(\sin\gamma)f_x+(\cos\gamma)f_y]^2\}\,,+\sin^2\beta(1-2\sin^2\gamma)f^2)\Big/\int dx\,dy\,|\,f\,|^2\,, \tag{26}$$

where β, γ, and ψ are determined variationally in previous sections. Both Eqs. (25) and (26) are analyzed variationally by making use of the ansatz wave function,

$$g(u)=e^{-\nu\cosh u},\quad f(u)=e^{-\mu\cosh u}\,. \tag{27}$$

We study the eigenvalues for both the uniform $\hat{d}$ case and the nonuniform $\hat{d}$ case. In the former case the eigenvalues, shown in Table I, depend weakly on r_0. In particular for $r_0/\xi_\perp\simeq 20$ the calculated transverse satellite frequency is in excellent agreement with that extrapolated to $T=T_c$ from the observed satellite frequency in the rotating superfluid ^{3}He-A; $\lambda_g=0.81$. Similarly the intensity of the resonance associated with a single pair of vortices is given by

$$I_t=\left\{\left|\int dx\,dy\,g\cos\psi\right|^2+\left|\int dx\,dy\,g\sin\psi\right|^2\right\}\Big/\int dx\,dy\,|\,g\,|^2 \tag{28}$$

TABLE II. Size parameter η, free energy f, and satellite resonance frequencies R_t and R_l of radial and circular vortices for variational functions $\cos\beta=e^{-(\eta r)^2}$ and $\cos\beta=e^{-\eta r}$.

		$\cos\beta=e^{-(\eta r)^2}$			$\cos\beta=e^{-\eta r}$		
Vortex	$\eta\xi_\perp$	f	R_t	R_l	f	R_t	R_l
Radial	$\sqrt{2/5}$	$5\ln r_0+2.435$	0.702	0.943	$5\ln r_0+1.927$	0.865	0.970
Circular	$\sqrt{2/3}$	$3\ln r_0+0.847$	0.935	0.997	$3\ln r_0-0.431$	0.971	0.999

and

$$I_l=\left|\int dx\,dy f\right|^2\Big/\int dx\,dy\,|f|^2, \tag{29}$$

for the transverse and the longitudinal modes. Again for corresponding r_0 the intensity is in good agreement with observation,[4] if we insert $\xi_\perp=10\ \mu$m, where $I_t^{\rm obs}$ is given by $I_t^{\rm obs}/I_0=0.058\Omega$, and I_0 is the intensity of the main peak in the absence of rotation. Now returning our attention to the case of nonuniform $\hat{d}$ texture, which is very likely to be realized in the parallel geometry, we obtain $\lambda_g=0.533$ and $\lambda_f=0.507$. This λ_g is much lower than that corresponding to the experimental value, although the results are somewhat better than those for the radial-hyperbolic vortex pair, which gives $\lambda_g=0.477$ and $\lambda_f=0.483$, respectively. Similarly, the calculated intensity for the transverse mode $I_t/I_0=0.071\Omega$ is somewhat larger than that observed experimentally. We do not understand this discrepancy, since in the parallel geometry the vortex pair with nonuniform $\hat{d}$ should be the equilibrium configuration, although the present texture cannot be the equilibrium texture when $\vec{H}$ is perpendicular to $\vec{\Omega}$. Perhaps the normal flow in the vortex flow may introduce additional perturbation, which has not been considered in the present analysis. Summing up the pure $\hat{l}$ texture appears to be more consistent with the experimental observation by Hakonen *et al.*[3,4] However, if it is the case the satellite frequency has a logarithmic dependence on Ω; as Ω increases the satellite frequency becomes lower, although this effect might be too small to be noticed. Furthermore, the pure $\hat{l}$ texture is more consistent with the tilted-field experiment, since the texture is unaffected by the field orientation. On the other hand, if the pure $\hat{l}$ texture is the case, it is quite puzzling why the nonuniform $\hat{d}$ texture is not realized for the parallel geometry where the nonuniform $\hat{d}$ texture is certainly more favored energetically. This clearly warrants further study on the vortex structure.

Note added in proof. (1) The sixth and eighth columns in Table I must be multiplied by a factor of 2. Thus the predicted I_t for the uniform $\hat{d}$ texture is roughly a factor of 2 larger than the observed value, while the nonuniform $\hat{d}$ texture gives a better agreement. (2) We have now extended our anlaysis to lower temperatures by making use of the generalized Ginzburg Landau free energy derived by Cross [M.C. Cross, J. Low Temp. Phys. **21**, 525 (1975)]. To our surprise we find that below $T<0.8T_c$ the transverse satellite frequency associated with the circular hyperbolic pair with nonuniform $\hat{d}$ agrees extremely well with the observed satellite frequency. Furthermore, the corresponding intensity is also fairly consistent with experiment. On the other hand, those due to the vortex pair with uniform $\hat{d}$ is far away from the observation. Therefore, the agreement between the uniform $\hat{d}$ texture with experiment found in this paper is fortuitous, perhaps due to the misleading extrapolation of the experimental data to $T=T_c$.

ACKNOWLEDGMENTS

Most of this work was done while we were staying at the Low Temperature Laboratory of Helsinki University of Technology (Otaniemi, Finland). We would like to thank the Low Temperature Laboratory for the hospitality during our stay. Particular thanks go to Martti Salomaa, Matti Krusius, and P. J. Hakonen for discussions on related subjects. One of us (K.M.) gratefully acknowledges support from Nordisk Institut for Teoretisk Atomphysik (NORDITA). The present work is supported by National Science Foundation under Grant No. DMR-82-14525.

APPENDIX A: ANALYSIS OF ISOLATED VORTICES

We limit ourselves here to the two types of analytic vortices, radial and circular. Since the vortex free energy is quite insensitive to the variation function chosen for the $\hat{d}$ vector for $\xi_H\ll\xi_\perp$, where ξ_H is the magnetic coherence length, we confine ourselves to the spatial dependence of $\cos\beta$ only. In I and II we have chosen $\cos\beta=e^{-(\eta r)^2}$ with η as a variational parameter. The vortex free energy for the radial and the circular vortex is given[1,2] as

$$f_r'=\int_0^{r_0} r\,dr\left[\frac{1}{r^2}(5-8\cos\beta+3\cos^2\beta)+(1+2\sin^2\beta)\beta_r^2+4\xi_\perp^{-2}\cos^2\beta\right] \tag{A1}$$

and

$$f_c'=\int_0^{r_0} r\,dr\left[\frac{1}{r^2}(3-8\cos\beta+5\cos^2\beta)+\beta_r^2+4\xi_\perp^{-2}\cos^2\beta\right], \tag{A2}$$

where $f'=f/\pi A$, and we have subtracted the contribution from the $\hat{d}$ texture. We have studied (A1) and (A2) for four types of variational functions $\cos\beta=e^{-(\eta r)^2}$, $e^{-\eta r}$, $(1+\alpha r)e^{-\alpha r}$, and $\mathrm{sech}(\alpha r)$. For the first two variational solutions the integrals are evaluated analytically. We find that the radial vortex $\cos\beta=(1-\alpha r)e^{-\alpha r}$, with $\alpha=1.342$, gives the best result $f_r'=5\ln(r_0/\xi_\perp)+1.921$, compared to the old value found in I with $\cos\beta=e^{-(\eta r)^2}$, $\eta=\sqrt{2/5}$,

and $f_r' = 5\ln(r_0/\xi_\perp)+2.435$, and the exact numerical result $f_r^{ex}=5\ln(r_0/\xi_\perp)+1.715$. On the other hand, the circular vortex is best approximated by $\cos\beta=e^{-\eta r}$, with $\eta=\sqrt{2/3}$ and $f_c' = 3\ln(r_0/\xi_\perp)-0.4312$, compared to the old value[1] $f_c' = 3\ln(r_0/\xi_\perp)+0.8472$. In both cases we find that $\cos\beta=e^{-\eta r}$ gives much lower vortex free energy than $\cos\beta=e^{-(\eta r)^2}$. We have recalculated the parameters in the satellite resonance frequencies $R_t=(\lambda_g)^{1/2}$ and $(\lambda_f)^{1/2}$, which are compared with the old results in Table II. We see immediately that in terms of better variational solutions, the circular-hyperbolic lattice is inconsistent with the experimental results. The radial-hyperbolic lattice may be more consistent with experiment, although this lattice cannot represent a possibility for the reason given in the text.

APPENDIX B: ANALYSIS OF THE RADIAL-HYPERBOLIC VORTEX PAIR

The radial-hyperbolic vortex is parametrized as follows:

$$\alpha=\phi_1+\phi_2,\quad \gamma=-\phi_1+\phi_2 \tag{B1}$$

and

$$\cos\psi=2(\sin^2 v)Y^{-1}-1\ , \tag{B2}$$

which are compared with Eqs. (5) and (16) in the text. Here we consider only the nonuniform $\hat{d}$ case for simplicity. Equations (B1) and (B2) are obtained from γ and ψ corresponding to the circular-hyperbolic vortex pair by rotating them by $\pi/2$ in the $\hat{x}$-$\hat{y}$ plane so that asymptotically $\hat{l}$ and $\hat{d}$ are now in the $\hat{x}$ direction far from the origin. We will not write the individual integrals here. But it is easy to see that the corresponding $I_1(f)$ and $I_2(f)$ are always larger than those for the circular-hyperbolic pair. Making use of a similar variation function for $\cos\beta=(\cos v)e^{-a(\cosh u-1)}$, and

$$Y=\theta^2+\sin^2 v\ , \tag{B3}$$

and θ given in Eq. (18), we find that

$$f_v=\pi A[12\ln(r_0/2C)+22.76]\ , \tag{B4}$$

for $a=0.7$, $b=1.2$, and $C=1.11\xi_\perp$.

APPENDIX C: INTEGRALS IN THE VORTEX FREE ENERGY

Substituting Eqs. (5), (7), and (17), where θ depends only on u, we obtain

$$I_1(f)=\frac{1}{2\pi}\int\int dx\,dy(4[\vec{\nabla}\alpha+(\cos\beta)\vec{\nabla}\gamma]^2+3\sin^2\beta(\vec{\nabla}\gamma)^2$$
$$-2\sin^2\beta\{[(\cos\gamma)\alpha_x-(\sin\gamma)\alpha_y]^2+[(\sin\gamma)\gamma_x+(\cos\gamma)\gamma_y]^2\})=I_{11}+I_{12}\ , \tag{C1}$$

where

$$I_{11}=\frac{1}{2\pi}\int\int du\,dv(4\{[\alpha_u+(\cos\beta)\gamma_u]^2+[\alpha_v(\cos\beta)\gamma_v]^2\}+3\sin^2\beta(\gamma_u^2+\gamma_v^2))$$
$$=\frac{2}{\pi}\int\int du\,dv\,X^{-1}\{4[\sinh^2 u+\cos^2 v-2(\cos^2 v)(\cosh u)f+(\cos^2 v)f^2]+3[1-(\cos^2 v)f^2]\}$$
$$=16\int_0^{u_0}du\{\tanh u+(\coth u-1)[1-2(\cosh u)f+f^2]\}+12\int_0^{u_0}\left[\frac{1-(\cosh^2 u)f^2}{\sinh u\cosh u}+f^2\right], \tag{C2}$$

and

$$I_{12}=-\frac{1}{\pi}\int\int du\,dv(\sin^2\beta)X^{-1}\left[\left[\cosh u\cos v+2-\frac{2(\cosh u\cos v+1)^2}{(\cosh u+\cos v)^2}\right]^2+4\sin^2 v\sinh^2 u\frac{(\cosh u\cos v+1)^2}{(\cosh u+\cos v)^2}\right]$$
$$=-\frac{4}{\pi}\int\int du\,dv[1-(\cos^2 v)f^2]X^{-1}\left[4+\cosh^2 u\cos^2 v-\frac{4(\cosh u\cos v+1)^3}{(\cosh u+\cos v)^2}\right]$$
$$=-8\left[\tfrac{1}{2}u_0+\tfrac{1}{4}-\ln 2+\int_0^{u_0}du\left[\frac{1}{\sinh u\cosh u}[1-(\cosh^2 u)f^2]+(\tfrac{13}{8}-\tfrac{5}{4}e^{-2u}+\tfrac{9}{8}e^{-4u}-\tanh)f^2\right]\right]. \tag{C3}$$

Finally combining I_{11} and I_{12}, we obtain $I_1(f)$ in Eq. (10) in the text. In the above analysis we made use of the following relations:

$$\sin\alpha=2\sinh u\cosh u\sin v\cos v\,X^{-1},\quad \cos\alpha=2\sinh^2 u\cos^2 v\,X^{-1}-1\ ,$$
$$\sin\gamma=1-2\sin^2 v\,X^{-1},\quad \cos\gamma=2\sinh u\sin v X^{-1}\ , \tag{C4}$$

and

$$\alpha_u = -2\sin v \cos v\, X^{-1},\quad \alpha_v = 2\sinh u \cosh u\, X^{-1},$$
$$\gamma_u = 2\cosh u \sin v\, X^{-1},\quad \gamma_v = -2\sinh u \cos v X^{-1}. \tag{C5}$$

Similarly $I_2(f)$ is obtained from

$$I_2(f) = \frac{1}{2\pi}\int\int du\, dv(\beta_u^2+\beta_v^2+2(\sin^2 v)(\sinh u - \cos v)^2 X^{-3}$$
$$\times\{[(\cosh u - \cos v)\cosh u - 2](\cos v) f_u + [(\cosh u - \cos v)\cos v + 2](\sinh u) f\}^2). \tag{C6}$$

Substituting

$$\beta_u = [1-(\cos^2 v) f^2]^{-1/2}(\cos v) f_u$$

and

$$\beta_v = -[1-(\cos^2 v) f^2]^{-1/2}(\sin v) f_v \tag{C7}$$

into (C6), the first two terms are easily integrated over v and we find Eq. (11) of the text. $I_3(f,b)$ can be rewritten as

$$I_3(f,b) = \frac{1}{\pi}\int dx\, dy\{(1+\cos^2\beta)\,|\,\nabla\psi\,|^2 + \sin^2\beta[(\sin\gamma)\psi_x + (\cos\gamma)\psi_y]^2\}$$
$$= \frac{1}{\pi}\int du\, dv[1+(\cos^2 v) f^2](\psi_u^2+\psi_v^2) + 4[1-(\cos^2 v) f^2] X^{-3} Y^{-2}\sin^2 v(\cosh u - \cos v)^2$$
$$\times\{[(\cosh u - \cos v)\cos v + 2](\sinh u)\theta_u + [(\cosh u - \cos u)\cosh u - 2](\cos v)\theta\}^2. \tag{C8}$$

Substituting

$$\psi_u = 2(\theta_u \sin v) Y^{-1},\quad \psi_v = -2(\theta\cos v) Y^{-1} \tag{C9}$$

where $Y = \theta^2 + \sin^2 v$, the first term in I_3 is evaluated as

$$I_{31} = \frac{4}{\pi}\int\int du\, dv[1-(\cos^2 v) f^2][(\sin^2 v)\theta_u^2 + \cos^2 v)\theta^2] Y^{-2}$$
$$= 4\int_0^\infty du\left\{\theta^{-1}(\theta^2+1)^{-1/2}[\theta_u^2(\theta^2+1)^{-1}+1] + 2\left[[(\theta^2+\tfrac{1}{2})\theta^{-1}(\theta^2+1)^{-1/2} - 1]\theta_u^2 + \left[\theta^2 - \frac{(\theta^2+\frac{1}{2})}{\theta}(\theta^2+1)^{1/2}\right] f^2\right]\right\}. \tag{C10}$$

Finally,

$$I_4(f,b) = \frac{1}{2\pi} C^2\int\int du\, dv X\left[1-[1-(\cos^2 v) f^2]\left[1 - \frac{4\sin^2 v}{X^2 Y^2}(\theta - \sinh u)^2(\theta\sinh u + \sin^2 v)^2\right]\right]$$
$$= \frac{1}{2\pi} C^2\int\int du\, dv\{C(\cos^2 v) f^2 + 4(\sin^2 v) X^{-1} Y^{-2}(\theta - \sinh u)^2(\theta\sinh u + \sin^2 v)^2[1-(\cos^2 v) f^2]\}. \tag{C11}$$

The first term in (C11) is easily integrated over v, which yields Eq. (21) in the text. For the pure $\hat{l}$ texture with uniform $\hat{d}$, we can take the limit θ tends to infinity. Then Eq. (21) reduces to Eq. (12) in the text.

---

[1] K. Maki, Phys. Rev. B **27**, 4173 (1983).
[2] K. Maki, Phys. Rev. B **28**, 2452 (1983).
[3] P. J. Hakonen, O. T. Ikkala, and S. T. Islander, Phys. Rev. Lett. **49**, 1258 (1983).
[4] P. J. Hakonen, O. T. Ikkala, S. T. Islander, O. V. Lounasmaa, and G. E. Volovik, J. Low Temp. Phys. **53**, 425 (1983).
[5] T. Fujita, M. Nakahara, T. Ohmi, and T. Tsuneto, Prog. Theor. Phys. **60**, 671 (1978).
[6] P. J. Hakonen and M. Krusius (private communication).
[7] H. K. Seppälä and G. E. Volovik, J. Low Temp. Phys. **51**, 279 (1983).
[8] P. W. Anderson and G. Toulouse, Phys. Rev. Lett. **38**, 508 (1977).
[9] H. K. Seppälä (private communication).